Antagonistic Roles of Neurofilament Subunits NF-H and NF-M Against NF-L in Shaping Dendritic Arborization in Spinal Motor Neurons

Jiming Kong, Vivian W.-Y. Tung, John Aghajanian, and Zuoshang Xu

Worcester Foundation for Biomedical Research, Department of Pharmacology and Molecular Toxicology, University of Massachusetts Medical Center, Shrewsbury, Massachusetts 01545

Abstract. Dendrites play important roles in neuronal function. However, the cellular mechanism for the growth and maintenance of dendritic arborization is unclear. Neurofilaments (NFs), a major component of the neuronal cytoskeleton, are composed of three polypeptide subunits, NF-H, NF-M, and NF-L, and are abundant in large dendritic trees. By overexpressing each of the three NF subunits in transgenic mice, we altered subunit composition and found that increasing NF-H and/or NF-M inhibited dendritic arborization, whereas increasing NF-L alleviated this inhibition. Examination of cytoskeletal organization revealed that increasing NF-H and/or NF-M caused NF aggregation and dissociation of the NF network from the microtubule (MT) network. Increasing NF-H or NF-H together with NF-M further reduced NFs from dendrites. However, these changes were reversed by elevating the level of NF-L with either NF-H or NF-M. Thus, NF-L antagonizes NF-H and NF-M in organizing the NF network and maintaining a lower ratio of NF-H and NF-M to NF-L is critical for the growth of complex dendritic trees in motor neurons.

Neurons are polarized cells that receive and integrate synaptic input on the surface of their dendrites and cell bodies, and conduct action potentials to distal targets via their axons. Ample evidence indicates that the neuronal cytoskeleton plays important roles in the development of neuronal polarity (Caceres and Kosik, 1990; Hirokawa, 1991; Caceres et al., 1992). Composed of three polypeptide subunits (NF-H, NF-M, and NF-L), neurofilaments (NFs)[1] belong to the intermediate filament family (Shaw, 1991) and are the most abundant cytoskeletal element in large neurons with long myelinated axons (Xu et al., 1994). Recent experiments have convincingly established that NFs play an indispensable role in the development and maintenance of normal axonal caliber (reviewed in Lee and Cleveland, 1996), a critical determinant of axonal conduction velocity (Arbuthnott et al., 1980). However, whether NFs also play a role in shaping the dendritic structure has not been explored.

Dendrites play an important role in neuronal function, particularly in neuronal plasticity (Yuste and Tank, 1996; Sejnowski, 1997). Dendrites create most of the surface area for synapse formation (Ulfhake and Kellerth, 1981; Brännström, 1993; Chen and Wolpaw, 1994), influence the integration of synaptic inputs and neuronal excitation (Mainen and Sejnowski, 1996; Magee and Johnston, 1997; Markram et al., 1997), and allow neurons to compartmentally regulate the distribution of a variety of cellular components, including cytoskeletal components (Kanai and Hirokawa, 1995; Kosik and Finch, 1987), ion channels, and receptors (Crino and Eberwine, 1996; Johnston et al., 1996). The highly diverse patterns of dendritic arborization reflect the unique connections and functions of the different neuronal populations. During development, the shape of each individual neuron is determined by a complex interaction between its genetic program and the surrounding environment (Purves and Lichtman, 1985). Consistent with its role in neuronal plasticity, the structure of dendrites remains plastic in both developing and mature neurons and is subject to modulation by neuronal activity, various neurotrophic factors and the size of target tissue (Greenough, 1984; Purves et al., 1986; Voyvodic, 1989; McAllister et al., 1996).

Thus, dendritic architecture is influenced by a variety of extrinsic factors. However, the intrinsic mechanism for the development and maintenance of dendritic architecture is relatively unexplored. The abundance of NFs in dendrites in many types of neurons (Peters et al., 1991) suggests that they may play a role in the growth and maintenance of elaborate dendritic trees. To investigate this possibility, we altered the NF subunit composition by selectively overexpressing each of the three NF subunits in transgenic mice

Address correspondence to Zuoshang Xu, Worcester Foundation for Biomedical Research, 222 Maple Avenue, Shrewsbury, MA 01545. Tel.: (508) 842-8921, ext. 255. Fax: (508) 842-3915. E-mail: xu@sci.wfbr.edu

1. *Abbreviations used in this paper*: MAP, microtubule-associated protein; MT, microtubule; NF, neurofilaments.

(Xu et al., 1996) and examined the dendritic architecture of spinal motor neurons. We found that an increased ratio of NF-H and/or NF-M to NF-L inhibited dendritic arborization, whereas a reduction in this ratio promoted it. Further examination of the cytoskeletal organization revealed that a high ratio of NF-H and NF-M to NF-L led to NF aggregation, dissociation of neurofilament and microtubule networks and depletion of NFs from dendrites. These results demonstrate that NF-H and NF-M play different roles from NF-L in organizing neuronal cytoskeleton and influencing dendritic growth. They also illustrate the importance of maintaining a lower ratio of NF-H and NF-M to NF-L during development, which favors the growth of neuronal processes.

Materials and Methods

Production of Transgenic Mice

Three transgenic lines that overexpress NF-L (line 58), NF-M-CΔ50 (line 42) and NF-H (line 35), have been produced and characterized in detail previously (Monteiro et al., 1990; Xu et al., 1993, 1996; Wong et al., 1995; Marszalek et al., 1996). All three lines express their transgene products at the highest level in spinal cord motor neurons. To produce mice overexpressing two NF subunits simultaneously, the three lines were intercrossed and transgenic mice carrying two transgenes: NF-L and NF-M, NF-L and NF-H, or NF-M and NF-H were determined by Southern blot as described previously (Xu et al., 1993, 1996; Wong et al., 1995; Marszalek et al., 1996). All mice used in this study were 17 d old.

Measurement of NF Protein Levels

Mice were killed at 17 d after birth and spinal cords were dissected and frozen immediately on dry ice. A piece of tail was saved from each mouse and used for transgene typing as described above. A quantitative Western blot described previously (Xu et. al., 1996) was used to quantify each NF subunits.

Tissue Preparation and Morphological Analysis

The rapid Golgi method was used as described in Morest (1981). Mice were fixed by transcardial perfusion using 4% paraformaldehyde in 0.1 M phosphate buffer (pH 7.4). A 0.3-cm segment of the lumbar enlargement of the spinal cord, centered at the attachment site of L5 ventral roots, was dissected out, immersed in 3% potassium bichromate and 1% osmium tetroxide for 3 d, and then stained with silver nitrate for 48 h. 70-μm transverse sections from the stained tissue was cut using a vibratome (TPI Inc., St. Louis, MO) and examined under a light microscope. Spinal cords that contained more than seven clearly stained motor neurons were further analyzed.

Motor neurons located within the anterior horn, with their cell bodies intact and larger than 30 μm in diameter, and with all the neurites clearly traceable, were drawn using a Nikon drawing tube at 300× magnification. The drawings were scanned into a computer using a HP ScanJet 3c. An equal number of neurons were then randomly selected from all the neurons drawn from each animal and measured using MetaMorph software (Universal Imaging Co., West Chester, PA). The number of neurons measured are 33 from 3 wild-type mice, 32 from 4 H mice, 21 from 3 M mice, 33 from 3 L mice, 20 from 2 HM mice, 20 from 2 LH mice, and 22 from 2 LM mice. The following definitions were used when measuring dendrites. Dendritic segment: the length of a dendrite between two branch points, between the cell body and the first branch point (primary dendrite), or the terminal segment that no longer branches. Dendritic tree: a primary dendrite and all the branches derived from it. The number of dendritic trees in a neuron equals the number of primary dendrites. Segment ratio: the ratio between the number of dendritic segments in the n^{th} + one order and that in the n^{th} order per neuron.

In these measurements, axons were not excluded because it was not possible to differentiate the axon from the dendrites in every neuron with full confidence. However, the inclusion of axons in the measurements of neurons with numerous and long dendrites was not expected to influence the results significantly because each neuron contains only one axon and the length of the axon is limited by sectioning. For neurons with significantly shortened dendrites, the contribution of an axon could be significant, and therefore, the measured dendritic length in these neurons would bias towards an overestimation. This would tend to diminish the difference between the wild-type and transgenic neurons. Despite this tendency, statistically significant differences were found between the wild-type and several transgenic lines (see Results).

To measure dendritic diameter and tapering, five neurons randomly selected from the above motor neuron pool were further drawn using 1,000× magnification. The diameters at both ends of each dendritic segment and the length of the dendritic segments were measured from the drawings. The proximal end of the primary dendrite was determined using the following criteria: the transitions from cell body membrane to dendrite membrane were located at points at which the membrane changed from convex out to concave out. A smooth convex arc consistent with the rest of the soma outline was drawn between the points and the midpoint of the arc was defined as the origin of primary dendrite (see Chen and Wolpaw, 1994). The average diameter of a segment was calculated as the average of the proximal and distal diameters. Dendritic tapering was the difference between the initial diameter and the end diameter of a dendritic segment per 100 μm of segment length. Rall's ratio was calculated from $(\Sigma[D_{daughter}^{3/2}])/(D_{parent}^{3/2})$ using the average diameter of dendritic segments. All statistical comparisons were carried out using Wilcoxon two-sample rank sum test.

For EM, mouse tissues were initially fixed by transcardial perfusion with a solution of 0.1 M sodium phosphate (pH 7.4), 4% paraformaldehyde, 2.5% glutaraldehyde, followed by further fixation in the same fixative for 24 h at 4°C. Tissues were then dissected out, postfixed with 2% osmium tetroxide in 0.1 M phosphate buffer, dehydrated in a graded ethanol series, and embedded in Epon-Araldite resin. 1-μm sections were stained with toluidine blue and examined by light microscopy. Thin sections were stained with uranyl acetate and lead citrate, examined and photographed in an electron microscope (model EM301; Philips Electron Optics, Mahwah, NJ).

Immunohistochemistry and Confocal Microscopy

Animals were perfused as described above using 4% paraformaldehyde in 0.1 M phosphate buffer. Spinal cords were dissected out and cut into 20-μm transverse sections with a vibratome. Sections were stained overnight at 4°C using a monoclonal antibody against MAP2 (a gift from Dr. R. Vallee; De Camilli et al., 1984) and a rabbit polyclonal antibody against NF-L (Xu et al., 1993). Rhodamine-conjugated goat anti–rabbit IgG and fluorescein-conjugated goat anti–mouse IgG (Jackson ImmunoResearch Laboratories Inc., West Grove, PA) were used as secondary antibodies. The doubly stained sections were examined with a scanning laser confocal microscope (model 1024; Bio-Rad Laboratories, Hercules, CA).

Results

Previous studies have shown that the three mouse lines (see Materials and Methods) overexpress each of the three NF subunits predominantly in spinal motor neurons (Wong et al., 1995; Marszalek et al., 1996; Xu et al., 1996). Measurements from 6-wk-old mice indicate an increase of two- to threefold of the endogenous levels (Wong et al., 1995; Marszalek et al., 1996; Xu et al., 1996). We measured the NF subunit levels in spinal cords of the 17-d-old animals. In each transgenic line, the respective NF subunit was increased (Table I), consistent with the previous measurements in sciatic nerves and ventral roots. However, some differences are noticeable in HM mice. In addition to large increases in the levels of NF-H and NF-M, NF-L level is also significantly increased (Table I), suggesting that increasing both NF-H and NF-M causes NF accumulation in motor neurons by hindering NF transport (see below).

To investigate the role of NFs in determining dendritic architecture, we stained spinal cord motor neurons using the Golgi method. Overexpression of each of the three NF subunits produced visually different patterns of dendritic

Table I. NF Subunit Content in Spinal Cord

	W	H	M	L	HM	HL	ML
NF-H	0.43 ± 0.12	1.35 ± 0.15	0.47 ± 0.12	0.46 ± 0.09	3.15 ± 0.32	1.78 ± 0.21	ND
NF-M	5.68 ± 0.71	4.93 ± 0.26	10.63 ± 0.47	6.30 ± 1.1	10.92 ± 0.69	4.81 ± 0.52	ND
NF-L	7.56 ± 0.73	8.19 ± 1.11	7.37 ± 0.86	13.01 ± 1.16	11.66 ± 0.95	11.66 ± 0.96	ND

NF subunit levels are expressed as pmol/100 μg total spinal cord protein. Each value is an average of three or more measurements ± SEM. The levels of NF-H are the sum of both phosphorylated and unphosphorylated forms.

arborization compared with the wild type (Fig. 1). Overexpression of either NF-H (H mice) or NF-M (M mice) shortened dendrites by ~60 and 30%, respectively, whereas overexpression of NF-L (L mice) did not cause a significant change (Figs. 1 and 2). The shortening caused by overexpression of either NF-H or NF-M was partially or completely alleviated by a simultaneous increase in the level of NF-L (compare H mice with LH mice and M mice with LM mice in Figs. 1 and 2). A simultaneous increase of both NF-H and NF-M nearly eliminated dendrites (Figs. 1 and 2).

To determine changes in dendritic branch pattern, we measured the number of dendritic trees, the length of each dendritic tree, the number of dendritic segments, and the length of dendritic segments in each neuron. Increasing NF-H reduced all of these parameters (Fig. 3). Increasing NF-M also reduced, to a less extent, three out of four parameters, with the number of dendritic segments per dendritic tree unaffected (Fig. 3). A combined increase of both NF-M and NF-H reduced all the parameters severely (Fig. 3). Although increasing NF-L alone did not affect any of these parameters (Fig. 3), when increased together with either NF-H or NF-M, NF-L was able to reverse partially or completely the reduction caused by increasing either subunit alone (Fig. 3). Interestingly, in the case of increasing NF-L together with NF-H, the reduction in the number of dendritic trees and dendritic segments (caused by increasing NF-H alone) was completely reversed. But this had no effect on the reduction of the length of dendritic tree and dendritic segments (compare H with LH in Fig. 3).

To further examine changes in dendritic branch patterns, we calculated the branch ratio at the successive dendritic branch points. Increasing either NF-H or NF-M reduced the third and fourth branches, while the second branches were unaffected (Fig. 4), indicating that the distal dendrites were affected. The reduction in the third branch number caused by increasing NF-H was not reversed by a simultaneous increase of NF-L (Fig. 4), despite the recovery of total number of dendritic segments per neuron to the normal level (Fig. 3). Whereas the third and fourth dendritic branches were not different from the wild type in L and LM mice, there was a significant increase in the second order dendritic branches, indicating that the proximal dendritic branches are increased. Increasing both NF-H and NF-M caused severe reduction in both proximal and distal dendritic branches.

To determine how dendritic diameters were affected by the altered neurofilament subunit composition, we measured segmental diameter, tapering and Rall's ratio. Increasing NF-H or both NF-H and NF-M caused a significant decrease in the diameter of the proximal dendrites but did not affect the diameter of the distal dendrites (Fig. 5). Increasing either NF-L or NF-M did not affect dendritic diameter significantly (Fig. 5). But increasing NF-L restored the reduced diameters of the proximal dendrites caused by increasing NF-H to normal (Fig. 5; compare *HL* with *H*). Altering NF subunit composition did not significantly affect dendritic tapering (Fig. 5). However, alteration of subunit composition by increasing any of the three subunits, with the exception of increasing NF-L, led to a reduction in Rall's ratio between the second and first order dendrites (Fig. 5).

To investigate how changes in NF subunit composition alter dendritic arborization, we examined the global organization of NFs and microtubules (MTs) by double immunofluorescence using an antibody against NF-L (Xu et al., 1993), in combination with antibodies against either microtubule-associated protein 2 (MAP2), which is distributed in cell bodies and dendrites (De Camilli et al., 1984) or class III β-tubulin (data not shown). Both combinations

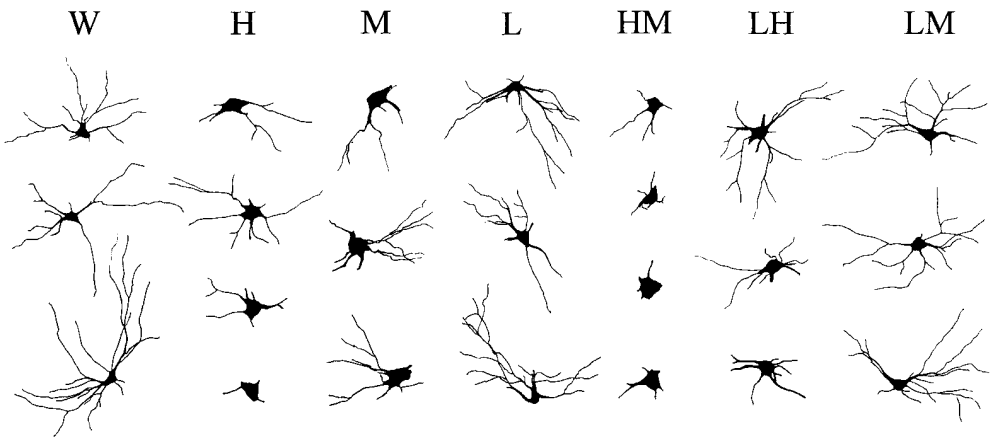

Figure 1. Camera lucida drawings of representative spinal motor neurons from mice transgenic for different NF subunits. All neurons are depicted at the same magnification. *W*, wild type; *H*, NF-H transgenic; *M*, NF-M transgenic; *L*, NF-L transgenic; *HM*, *LH*, and *LM*, represent the mice that are doubly transgenic for two subunits.

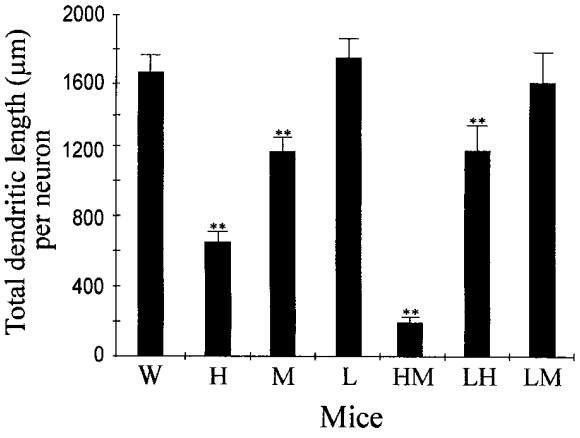

Figure 2. Changes in the average total dendritic length per motor neuron. The length of dendrites was measured for each neuron and the average length per neuron was calculated for each transgenic line. Error bars represent SEM Single and double stars represent the values that were significantly different ($P < 0.05$ and $P < 0.01$, respectively) from that of the wild type.

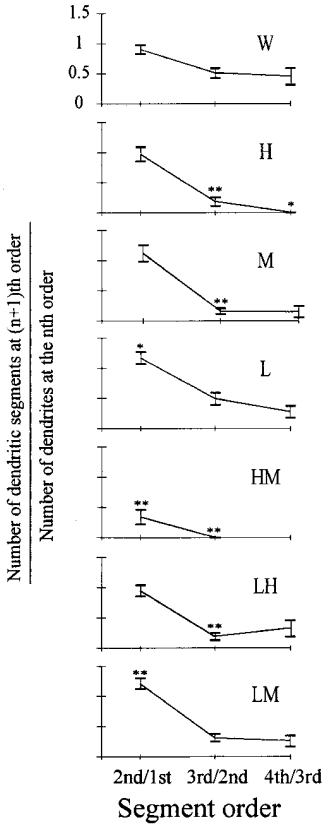

Figure 4. Changes in dendritic branch pattern. Dendritic branches are evaluated by calculating the ratio of dendritic segments in successive dendritic order (see Materials and Methods). The ratio beyond the fourth order were not calculated because of low segment numbers. Symbols are the same as in Figs. 1 and 2.

revealed the same pattern in wild-type motor neurons: both NFs and microtubules were organized into elaborate networks, which extended well into the dendrites (Fig. 6, *A* and *B*, *arrows*). A close alignment between NF and MT networks was also evident, as indicated by a substantial overlap between the two networks (Fig. 6, *A–C*).

The close alignment between the NF and MT networks was altered by an increase in NF-M. Instead of forming an intricate network, NFs appeared bundled together (Fig. 6 *D*, *arrowheads*), with some of these bundles excluding microtubules (Fig. 6, *E* and *F*, *arrowheads*). Although the extension of both NFs and microtubules into the proximal dendrites was not affected (Fig. 6, *D–F*, *large arrows*), the NF content in distal dendrites appeared decreased, as indicated by the reduced NF staining in small dendritic segments (Fig. 6, *D–F*, *small arrows*). Both aggregation of NFs and dissociation of NF and MT networks were further aggravated by the elevated expression of NF-H (Fig. 6, *G–I*, *arrowheads*), resulting in a depletion of NFs from distal

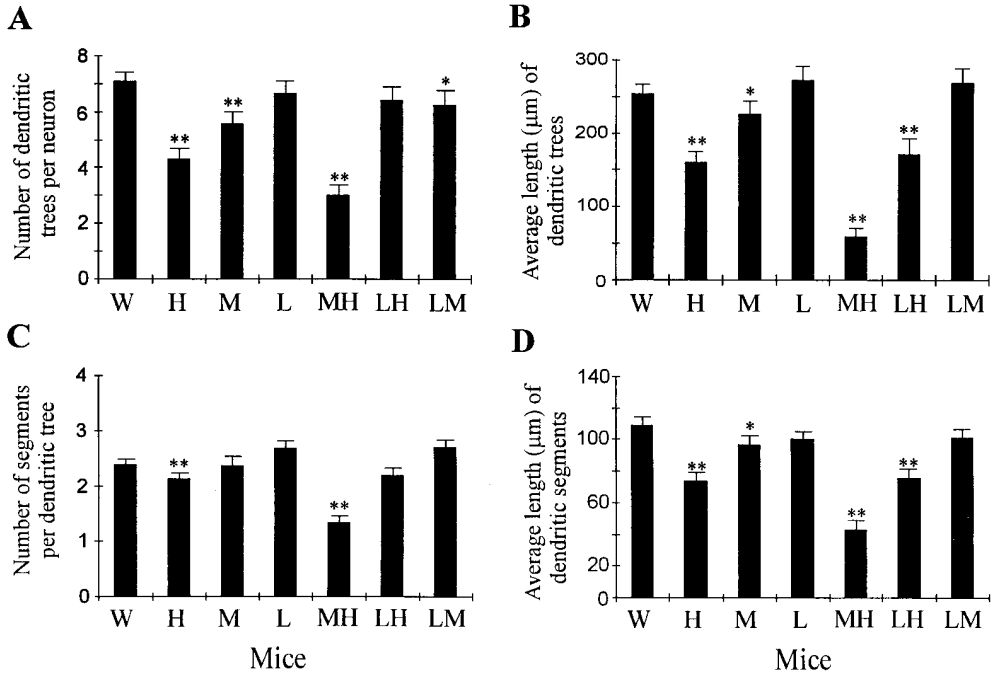

Figure 3. Changes in the dendritic structure caused by changes in NF subunit composition. Values were measured from each neuron and then averaged for each transgenic line. Symbols are the same as in Figs. 1 and 2. The definitions for dendritic tree and dendritic segments are described in Materials and Methods.

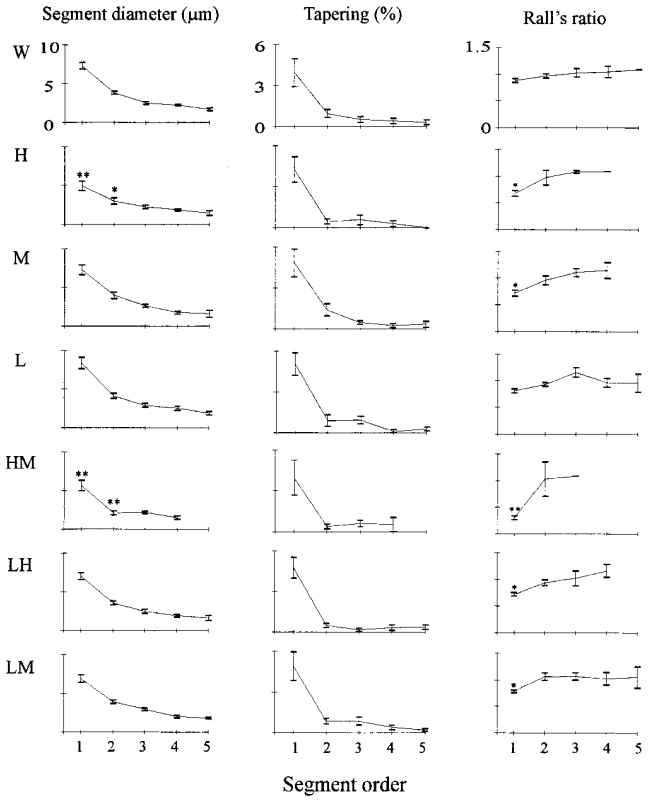

Figure 5. Changes in dendritic diameter, tapering, and Rall's ratio (see Materials and Methods). Symbols are the same as in Figs. 1 and 2.

(Fig. 6, *G–I*, *small arrows*) and proximal dendrites (Fig. 6, *G–I*, *large arrows*) and dendritic attrition (Fig. 6, *G–I*, *large arrows*). In contrast to these effects, increasing NF-L did not cause aggregation of NFs or dissociation between NF and MT networks, nor did it lead to NF depletion from proximal dendrites or dendritic atrophy (Fig. 6, *J–L*, *arrows*). These results suggest that NF-L plays a role antagonistic to NF-H and NF-M and that a balanced ratio among these subunits is crucial to maintaining the cytoskeletal organization in neurons.

To confirm this point, we examined the cytoskeletal organization in mice that overexpress two subunits simultaneously. Increasing NF-L together with either NF-M or NF-H prevented the formation of NF aggregates and the dissociation of NF and MT networks (Fig. 7, *A–F*). Most notably, it prevented the depletion of NFs from dendrites (Fig. 7, *D–F*, *arrows*) that was caused by increasing NF-H alone (Fig. 6, *G–I*, *arrows*). Thus, increasing NF-L reverses the alterations in cytoskeletal organization caused by increasing NF-H and NF-M despite a further increase in the total NF protein content (Table I). In contrast to the role of increasing NF-L, increasing both NF-M and NF-H caused the most severe aggregation of NFs (Fig. 7, *G–I*, *arrowheads*) and depletion of NFs from dendrites and dendritic attrition (Fig. 7, *G–I*, *arrows*). Thus, a high ratio of NF-H and NF-M to NF-L, rather than an increase in the total amount of NF polypeptides, leads to the alteration in cytoskeletal organization and dendritic arborization.

To determine the nature of the NF aggregates, motor neurons were examined using EM. In neurons from the wild-type mice, various cellular organelles, including NFs and MTs, were interspersed throughout the cytoplasm (Fig. 8 *A*). This cytoplasmic organization was altered in neurons that express high levels of NF-H, NF-M, or both NF-H and NF-M. All of these neurons had NF aggregates that were composed of large parallel filament bundles (Fig. 8, *B*, *C*, and *E*). These bundles were separated from the cell and nuclear membrane by a layer of other cytoplasmic organelles (Fig. 8, *B*, *C*, and *E*). These nonfilamentous cytoplasmic layers were connected by several tracks, which contain MTs and various other organelles (Fig. 8, *B*, *C*, and *E*, between arrowheads) that correlate with the regions stained positively with MAP2 and tubulin antibodies, including the cell periphery, the perinuclear region and the thin tracks connecting these two regions (Figs. 6, *E* and *H* and 7 *H*).

In contrast to increasing NF-H and NF-M, increasing NF-L led to an increase in NF bundles that traverse among small islands of RER and other cellular organelles, but did not cause large filament aggregation (Fig. 8 *D*). NFs were also distributed in close proximity of cell and nuclear membrane (Fig. 8 *D*). When NF-L was increased together with NF-H, the formation of NF aggregates caused by increasing NF-H alone was prevented (compare Fig. 8, *B* with *F*). The same results were also observed when NF-L was increased together with NF-M (data not shown).

To determine how changes in NF subunit composition affected NF distribution in dendrites, and in particular, to find out how neurofilament network was disrupted abruptly in the proximal dendrites, we further examined dendritic initiation zone using EM. In wild-type mice there were abundant neurofilaments in dendrites (Fig. 9, *A* and *B*). They formed parallel bundles and were a continuous extension of the NF network in the cell body (Fig. 9, *A* and *B*). In sharp contrast, the NFs forming aggregates in the cell body in H (Fig. 9, *C* and *D*) or HM mice (Fig. 9, *G* and *H*) failed to extend into the proximal dendrites, leaving mostly microtubules in the proximal dendrites. The disrupted extension of NFs into the proximal dendrites caused by an increase in NF-H was reversed by increasing NF-L (Fig. 9, *I* and *J*). In M (Fig. 9 *E*), L (Fig. 9 *F*), and LM (not shown) mice the number of NFs was increased in the proximal dendrites and the continuous extension of the NF network from the cell body to the proximal dendrites was not affected.

Discussion

This study demonstrates the distinct effects of different NF subunits on cytoskeletal organization and dendritic structure in spinal motor neurons. Increasing NF-H, NF-M, or both subunits led to NF aggregation and a segregation of the NF network from the MT network (Figs. 6–9). These effects were more severe in the case of increasing NF-H or both NF-H and NF-M, leading to a drastic reduction of NFs in dendrites (Figs. 6, 7, 9). Increasing NF-L, however, reversed these changes and led to a close association between the NF and MT networks and an extension of NFs into dendrites (Figs. 6–9). Correlating with these changes, increasing NF-H and/or NF-M inhibited dendritic arborization, whereas increasing NF-L alleviated this re-

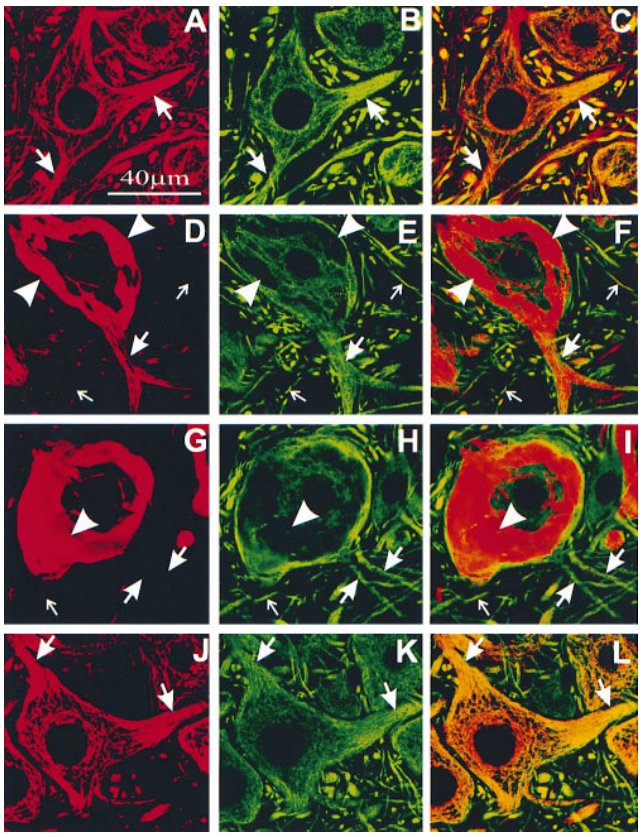

Figure 6. Different effects of overexpressing each of the three NF subunits on cytoskeletal organization. Spinal motor neurons were doubly stained with antibodies against NF-L (*red*) and MAP2 (*green*). The third column shows the superimposed images of both stains. (*A–C*) Wild type; (*D–F*) M mice; (*G–I*) H mice; (*J–L*) L mice. Arrowheads point to NF aggregates and arrows point to dendrites.

duction (Figs. 1–4). These results demonstrate that NF-H and NF-M antagonize NF-L in organizing the NF network and dendritic growth and that a lower ratio of NF-H and/or NF-M to NF-L is required for the growth of elaborate dendritic trees. This finding sheds light on the significance of the developmental regulation of NF subunit expression (see below).

Previous experiments have shown that a high ratio of NF-H and NF-M to NF-L inhibited radial axonal growth (Wong et al., 1995; Marszalek et al., 1996; Xu et al., 1996). Our current efforts demonstrate that the high ratio is also inhibitory to dendritic growth, thus proving that a high ratio of NF-H and NF-M to NF-L is generally inhibitory to neuronal process growth. Our observations suggest that this inhibition is derived from interference with the interaction between NF and MT networks by the increased ratio of NF-H and/or NF-M to NF-L that leads to a dissociation of the NF and MT networks (Figs. 6–8). Because long distance intracellular organelle transport is known to be microtubule dependent (Vallee and Bloom, 1991), such a dissociation could lead to an inhibition of NF transport, resulting in a decreased NF content in both axons and dendrites (Wong et al., 1995; Marszalek et al., 1996; Xu et al., 1996; Figs. 6, 7, 8) and an accumulation of NFs in cell bodies (Fig. 8).

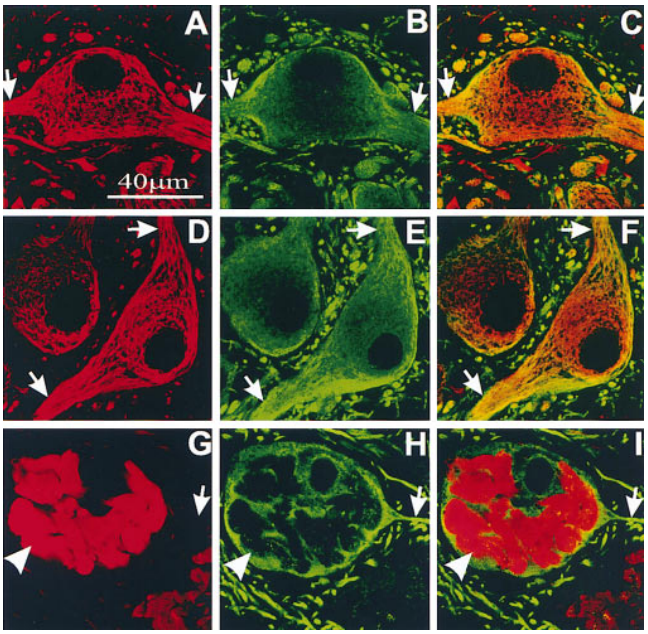

Figure 7. Overexpression of NF-L prevents whereas overexpression of NF-H and NF-M induces NF aggregation. Spinal motor neurons were doubly stained with antibodies against NF-L (*red*) and MAP2 (*green*). The third column shows the superimposed images of both stains. (*A–C*) LM mice; (*D–F*) LH mice; (*G–I*) HM mice. Arrowheads point to NF aggregates and arrows point to dendrites.

A close association of intermediate filaments and MTs in cultured cells has been widely observed and disruption of this interaction leads to a collapse of intermediate filament network into aggregates (Blose et al., 1984; Gyoeva and Gelfand, 1991). We show that NFs are closely associated with MTs in neurons in vivo. The dissociation of NFs from MTs and the formation of NF aggregates after the increased ratio of NF-H and/or NF-M to NF-L suggest that NF-H and NF-M weaken the association of NFs with MTs and promote NF self association. The reversal of this dissociation and NF aggregation by an increase in NF-L suggests that NF-L plays an interactive role between NFs and MTs. Candidates for mediating this interaction include microtubule associated proteins, such as MAP2 and tau. Both have been shown to bind to microtubules as well as NF-L in vitro (Heimann et al., 1985; Miyata et al., 1986). Other potential mediators include microtubule-based motors (Gyoeva and Gelfand, 1991) and the intermediate filament-associated protein plectin (Svitkina et al., 1996).

The mechanism for the inhibition of the interaction between NFs and MTs by the high ratio of NF-H and/or NF-M to NF-L is not clear. One possibility is that an increased ratio of NF-H and/or NF-M to NF-L may increase the density of their COOH-terminal tails projecting from the filament core where NF-L resides (Hirokawa et al., 1984; Hirokawa, 1991). Because NF-L may play an interactive role with MTs, a high density of NF-H and NF-M tails could block this interaction due to stereo hindrance. Concomitant with inhibiting the interaction between NFs and MTs, NF-H and NF-M may also promote self-association among NFs (Xu et al., 1996), mediated by their COOH-terminal tails of these molecules (Hirokawa et al., 1984;

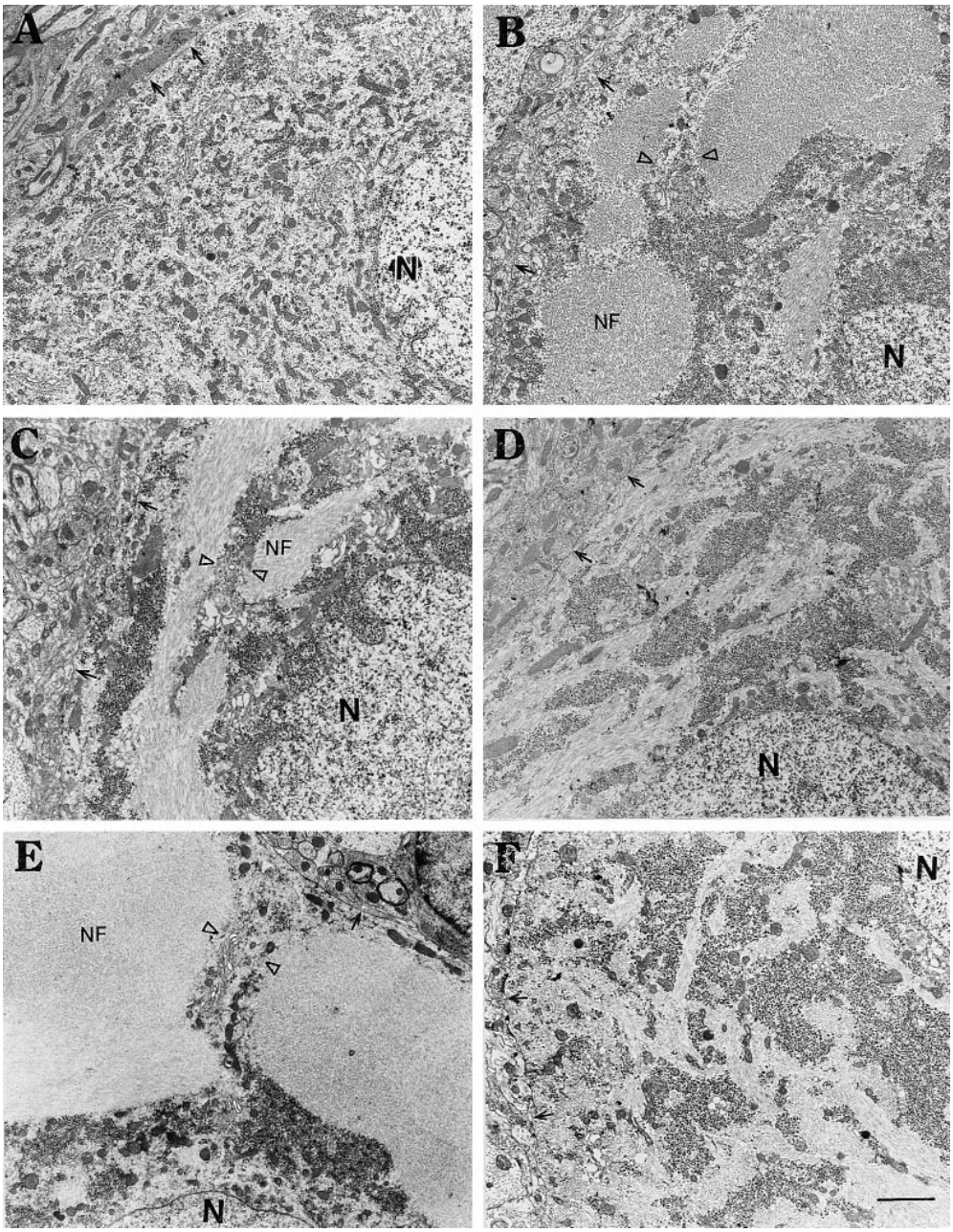

Figure 8. Changes in NF network and cytoplasmic organization in motor neurons overexpressing different NF subunits. Spinal motor neurons were photographed with EM and displayed at the same magnification. (*A*) Wild type, (*B*) H mice, (*C*) M mice, (*D*) L mice, (*E*) HM mice, and (*F*) LH mice. NF marks NF aggregates; arrows point to cytoplasmic membrane; arrowheads point to tracks connecting the perinuclear and the peripheral cytoplasmic regions. Bar, 2.5 μm.

Hirokawa, 1991). Thus, both interference with the interaction between NFs and MTs and a tendency for self-association may contribute to the formation of NF aggregates when the ratio of NF-H and/or NF-M to NF-L is increased. By the same token, increasing NF-L lowers the density of NF-H and NF-M tails, which in turn reduces the stereo hindrance, therefore allowing the interaction between NFs and MTs to occur.

The reduced NF content in dendrites as a consequence of an increased ratio of NF-H and NF-M to NF-L is consistent with a reduction in transport of NFs into neuronal processes and is a likely cause that leads to structural changes in dendrites. These changes include reductions in diameter of proximal dendrites (Fig. 5), the number of primary dendrites (Fig. 3 *A*), distal dendritic branching (Fig. 4) and the length of dendritic segments (Fig. 3 *D*). Although increasing NF-L alone does not affect most of these parameters, when increased together with NF-H or NF-M, it partially or completely alleviated the reduction in these dendritic parameters (Figs. 1–5). The most dramatic effects are in the recovery of proximal dendritic diameter and the number of primary dendrites in LH mice (Figs. 5 and 3 *A*). Coincident with these recoveries is the recovery of NF content in the proximal dendrites (Figs. 7, *D–F* and 9, *I* and *J*). Interestingly, recovery of the length of dendritic segments (Fig. 3, *A* and *D*) is not observed and the recovery of distal dendritic branching is incomplete in LH mice (Fig. 4), suggesting that the effect of increasing NF-L is limited to the proximal dendrites.

In a mathematical simplification of the electrical properties of complex dendritic arborization, Rall used a single element or equivalent cylinder to describe a dendritic tree

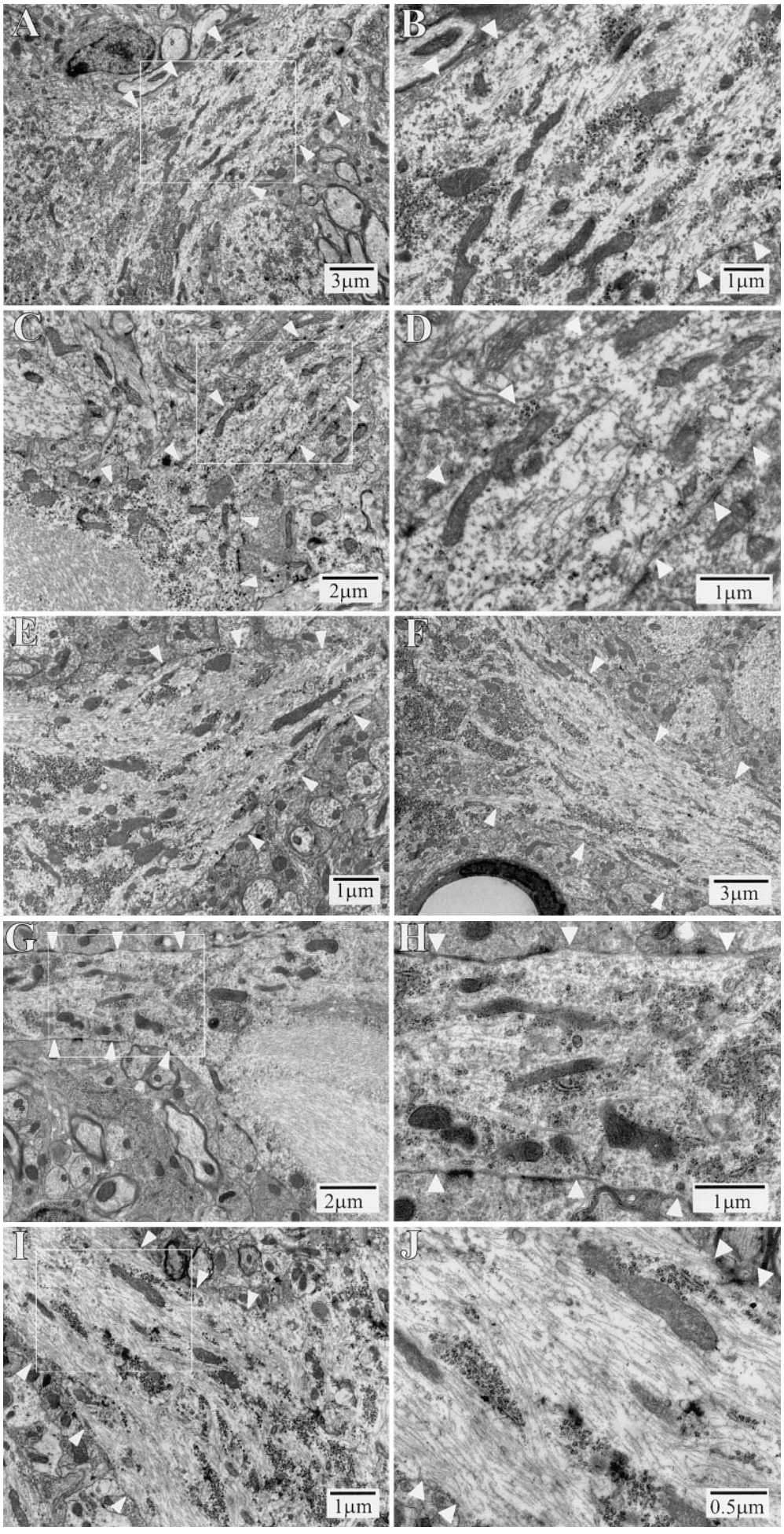

Figure 9. NF distribution in the proximal dendrites. (*A* and *B*) Wild type; (*C* and *D*) H mice; (*E*) M mice; (*F*) L mice; (*G* and *H*) MH mice; (*I* and *J*) LH mice. Arrowheads points to cytoplasmic membrane at the initial segment of dendrites.

(Rall, 1995). Rall's ratio is a constraint in this model that requires $(\Sigma[D_{daughter}^{3/2}])/(D_{parent}^{3/2}) = 1$ (D represents diameter of dendritic segments). Our results show a Rall's ratio being close to one in wild-type mice, agreeing with other studies (Ulfhake and Kellerth, 1981; Brännström, 1993; Chen and Wolpaw, 1994). Changes in NF subunit composition do not lead to a significant deviation from the Rall's ratio in the overall dendritic structure. Only the ratio between the second and the first order dendrites is reduced in all except L mice, whereas the ratios in distal dendrites are unaffected (Fig. 5).

These findings shed light on the developmental regulation of NF subunit expression. The expression of NF-L and NF-M closely follows neuronal differentiation (Carden et al., 1987; Kost et al., 1992) and is associated with the earliest stages of neuronal process growth (Cochard and Paulin, 1984; Landmesser and Swain, 1992; Crino and Eberwine, 1996). However, the expression of NF-H does not increase significantly until >10 d after birth (Shaw and Weber, 1982; Pachter and Liem, 1984). Whereas the coexpression of NF-L and NF-M during the early stages of development is consistent with the finding that at least two subunits, composed of NF-L and either NF-M or NF-H, are required for NF assembly in cells (Ching and Liem, 1993; Lee et al., 1993), maintaining a low level of NF-H may be important for dendritic growth. On this note, it is interesting to notice that at age 17 d, the ratio of NF-H to NF-L in wild-type mice is 0.06 (Table I), approximately threefold lower than the ratio in 6-wk-old mice (Xu et. al., 1996). Increasing NF-H in H mice brings the ratio to 0.16 (Table I). This ratio is similar to that in 6-wk-old animals (Xu et. al., 1996), yet it produces a remarkable inhibition of dendritic arborization (Figs. 1–5). Thus, our current results indicate that the delayed expression of NF-H enables dendritic growth.

The outcome of this study raises the question of why the ratio of NF-H to NF-L increases as neurons develop to maturity. The early appearance and enrichment of NF-L and NF-M in neuronal processes suggests that NFs play a role in the early development of these processes (Cochard and Paulin, 1984; Landmesser and Swain, 1992; Crino and Eberwine, 1996). On the other hand, neuronal maturation correlates with an increase in NF-H and slowing of axonal transport (Willard and Simon, 1983). Therefore, the increase in the level of NF-H may increase the stability of cytoskeleton and thereby stabilize neuronal structure in mature neurons (Willard and Simon, 1983). Collectively, the existing experimental data suggests the following sequence of events during development: as NF-H increases, the interaction between NFs and microtubules weakens, and the interaction among NFs themselves strengthens. This leads to an extensive cross-bridge formation among NFs (Hirokawa et al., 1984) and slower transport of cytoskeletal components (Willard and Simon, 1983). As these changes proceed, a stable NF matrix within axons and dendrites (particularly proximal dendrites) is formed and neuronal processes stabilize. Thus, neurons may regulate the ratio of NF-H to NF-L in order to maintain a balance between plasticity and stability of neuronal processes during different stages of development. Such a process is perhaps most relevant in large NF-rich neurons with long axons and long dendrites radiating from their cell bodies (such as motor neurons and Betz cells). The role of neurofilaments in the development of dendritic trees with short branches may be less significant. Consistent with this view, small neurons that do not have long dendritic trees and large neurons with numerous but short segmental dendritic branches (e.g., Purkinje cells) express little neurofilaments. Taken together, our results show that NFs play an important role in the development of large dendritic trees with long segmental branches.

We thank Diane Casey and Curt Wilkerson for critically reading the manuscript, Richard Vallee for providing MAP2 antibody and discussion. This work was supported by National Institute of Health and Lucillle P. Markey Charitable Trust.

Received for publication 1 August 1997 and in revised form 5 January 1998.

References

Arbuthnott, E.R., I.A. Boyd, and K.U. Kalu. 1980. Ultrastructural dimensions of myelinated peripheral nerve fibres in the cat and their relation to conduction velocity. *J. Physiol.* 308:125–157.

Blose, S.H., D.I. Meltzer, and J.R. Feramisco. 1984. 10-nm filaments are induced to collapse in living cells microinjected with monoclonal and polyclonal antibodies against tubulin. *J. Cell Biol.* 98:847–858.

Brännström, T. 1993. Quantitative synaptology of functionally different types of cat medial gastrocnemius a-motoneurons. *J. Comp. Neurol.* 330:439–454.

Caceres, A., and K.S. Kosik. 1990. Inhibition of neurite polarity by tau antisense oligonucleotides in primary cerebellar neurons. *Nature*. 343:461–463.

Caceres, A., J. Mautino, and K.S. Kosik. 1992. Suppression of MAP2 in cultured cerebellar macroneurons inhibits minor neurite formation. *Neuron*. 9:607–618.

Carden, M.J., J.Q. Trojanowski, W.W. Schlaepfer, and V.M.-Y. Lee. 1987. Two-stage expression of neurofilament polypeptides during rat neurogenesis with early establishment of adult phosphorylation patterns. *J. Neurosci.* 7:3489–3504.

Chen, X.Y., and J.R. Wolpaw. 1994. Triceps surae motoneuron morphology in the rat: a quantitative light microscopic study. *J. Comp. Neurol.* 343:143–157.

Ching, G., and R. Liem. 1993. Assembly of type IV neuronal intermediate filaments in nonneuronal cells in the absence of preexisting cytoplasmic intermediate filaments. *J. Cell Biol.* 122:1323–1335.

Cochard, P., and D. Paulin. 1984. Initial expression of neurofilaments and vimentin in the central and peripheral nervous system of the mouse embryo in vivo. *J. Neurosci.* 4:2080–2094.

Crino, P.B., and J. Eberwine. 1996. Molecular characterization of the dendritic growth cone: regulated mRNA transport and local protein synthesis. *Neuron*. 17:1173–1187.

De Camilli, P., P.E. Miller, F. Navone, W.E. Theurkauf, and R.B. Vallee. 1984. Distribution of microtubule-associated protein 2 in the nervous system of the rat studied by immunofluorescence. *J. Neurosci.* 11:819–846.

Greenough, W.T. 1984. Structural correlates of information storage in the mammalian brain: a review and hypothesis. *Trends Neurosci.* 7:229–233.

Gyoeva, F.K., and V.I. Gelfand. 1991. Coalignment of vimentin intermediate filaments with microtubules depends on kinesin. *Nature*. 353:445–448.

Heimann, R., M.L. Shelanski, and R.K.H. Liem. 1985. Microtubule-associated proteins bind specifically to the 70-kDa neurofilament protein. *J. Biol. Chem.* 260:12160–12166.

Hirokawa, N. 1991. Molecular architecture and dynamics of the neuronal cytoskeleton. *In* The Neuronal Cytoskeleton. R.D. Burgoyne, editor. Wiley-Liss, Inc., New York. 5–74.

Hirokawa, N., M.A. Glicksman, and M.B. Willard. 1984. Organization of mammalian neurofilament polypeptides within the neuronal cytoskeleton. *J. Cell Biol.* 98:1523–1536.

Johnston, D., J.C. Magee, C.M. Colbert, and B.R. Christie. 1996. Active properties of neuronal dendrites. *Annu. Rev. Neurosci.* 19:165–186.

Kanai, Y., and N. Hirokawa. 1995. Sorting mechanisms of tau and MAP2 in neurons: suppressed axonal transit of MAP2 and locally regulated microtubule binding. *Neuron*. 14:421–432.

Kosik, K.S., and E.A. Finch. 1987. MAP2 and Tau segregate into dendritic and axonal domains after the elaboration of morphologically distinct neurites: an immunocytochemical study of cultured rat cerebrum. *J. Neurosci.* 7:3142–3153.

Kost, S.A., K. Chacko, and M.M. Oblinger. 1992. Developmental patterns of intermediate filament gene expression in the normal hamster brain. *Brain Res.* 595:270–280.

Landmesser, L., and S. Swain. 1992. Temporal and spatial modulation of a cytoskeletal antigen during peripheral axonal pathfinding. *Neuron*. 8:291–305.

Lee, M.K., and D.W. Cleveland. 1996. Neuronal intermediate filaments. *Annu. Rev. Neurosci.* 19:187–217.

Lee, M.K., Z.-S. Xu, P.W. Wong, and D.W. Cleveland. 1993. Neurofilaments are obligate heteropolymers in vivo. *J. Cell Biol.* 122:1337–1350.
Magee, J.C., and D. Johnston. 1997. A synaptically controlled, associative signal for Hebbian plasticity in hippocampal neurons. *Science*. 275:208–213.
Mainen, Z.F., and T.J. Sejnowski. 1996. Influence of dendritic structure on firing pattern in model neocortical neurons. *Nature*. 382:363–366.
Markram, H., J. Lübke, M. Frotscher, and B. Sakmann. 1997. Regulation of synaptic efficacy by coincidence of postsynaptic APs and EPSPs. *Science*. 275:213–215.
Marszalek, J.R., T.L. Williamson, M.K. Lee, Z.-S. Xu, P.N. Hoffman, M.W. Becher, T.O. Crawford, and D.W. Cleveland. 1996. Neurofilament subunit NF-H modulates axonal diameter by selectively slowing neurofilament transport. *J. Cell Biol.* 135:711–724.
McAllister, A.K., L.C. Katz, and N.C. Lo. 1996. Neurotrophin regulation of cortical dendritic growth requires activity. *Neuron*. 17:1057–1064.
Miyata, Y., M. Hoshi, E. Nishida, Y. Minami, and H. Sakai. 1986. Binding of microtubule-associated protein 2 and tau to the intermediate filament reassembled from neurofilament 70-kDa subunit protein. *J. Biol. Chem.* 261: 13026–13030.
Monteiro, M.J., P.N. Hoffman, J.D. Gearhart, and D.W. Cleveland. 1990. Expression of NF-L in both neuronal and nonneuronal cells of transgenic mice: increased neurofilament density in axons without affecting caliber. *J. Cell Biol.* 111:1543–1557.
Morest, D.K. 1981. The Golgi methods. *In* Techniques in Neuroanatomical Research. C. Heym and W.-G. Forssmann, editors. Springer-Verlag, Berlin. 124–138.
Pachter, J.S., and R.K.H. Liem. 1984. The differential appearance of neurofilament triplet polypeptides in the developing rat optic nerve. *Dev. Biol*. 103:200–210.
Peters, A., S.L. Palay, and H.D. Webster. 1991. The fine structure of the nervous system. Oxford University Press, New York. pp. 494.
Purves, D., and J.W. Lichtman. 1985. Principles of Neural Development. Sinauer Associates Inc., Sunderland, MA. pp. 433.
Purves, D., R.D. Hadley, and J.T. Voyvodic. 1986. Dynamic changes in the dendritic geometry of individual neurons visualized over periods of up to three months in the superior cervical ganglion of living mice. *J. Neurosci.* 6:1051–1060.
Rall, W. 1995. The Theoretical Foundation of Dendritic Function. I. Segev, J. Rinzel, and G.M. Shepherd, editors. MIT Press, Cambridge, MA. pp. 470.
Sejnowski, T.J. 1997. The year of the dendrite. *Science*. 275:178–179.
Shaw, G. 1991. Neurofilament proteins. *In* The Neuronal Cytoskeleton. R.D. Burgoyne, editor. Wiley-Liss, Inc., New York. 621–635.
Shaw, G., and K. Weber. 1982. Differential expression of neurofilament triplet proteins in brain development. *Nature*. 298:277–279.
Svitkina, T.M., A.B. Verkhovsky, and G.G. Borisy. 1996. Plectin sidearms mediate interaction of intermediate filaments with microtubules and other components of the cytoskeleton. *J. Cell Biol.* 135:991–1007.
Ulfhake, B., and J.-O. Kellerth. 1981. A quantitative light microscopic study of the dendrites of cat spinal a-motoneurons after intracellular staining with horseradish peroxidase. *J. Comp. Neurol.* 202:571–583.
Vallee, R.B., and G.S. Bloom. 1991. Mechanisms of fast and slow axonal transport. *Annu. Rev. Neurosci.* 14:59–92.
Voyvodic, J.T. 1989. Peripheral target regulation of dendritic geometry in the rat superior cervical ganglion. *J. Neurosci.* 9:1997–2010.
Willard, M., and C. Simon. 1983. Modulation of neurofilament axonal transport during the development of rabbit retinal ganglion cells. *Cell*. 35:551–559.
Wong, P.C., J.R. Marszalek, T.O. Crawford, Z.-S. Xu, S.-T. Hsieh, J.W. Griffin, and D.W. Cleveland. 1995. Increasing NF-M expression reduces axonal NF-H, inhibits radial growth and results in neurofilamentous accumulation similar to that found in human motor neuron disease. *J. Cell Biol.* 130:1413–1422.
Xu, Z.-S., L.C. Cork, J.W. Griffin, and D.W. Cleveland. 1993. Increased expression of neurofilament subunit NF-L produces morphological alterations that resemble the pathology of human motor neuron disease. *Cell*. 73:23–33.
Xu, Z.-S., D.L.-Y. Dong, and D.W. Cleveland. 1994. Neuronal intermediate filaments: new progress on an old subject. *Curr. Opin. Neurobiol.* 4:655–661.
Xu, Z.-S., J.R. Marszalek, M.K. Lee, P.C. Wong, T.O. Crawford, S.-T. Hsieh, J.W. Griffin, and D.W. Cleveland. 1996. Subunit composition of neurofilaments specifies axonal diameter. *J. Cell Biol.* 133:1061–1070.
Yuste, R., and D.W. Tank. 1996. Dendritic integration in mammalian neurons, a century after Cajal. *Neuron*. 16:701–716.